Heterocyclic reactive mesogens: synthesis, characterisation and mesomorphic behaviour

Matthew P. Aldred[a]; Panos Vlachos[a]; Dewen Dong[b]; Stuart P. Kitney[a]; W. Chung Tsoi[c]; Mary O'Neill[c]; Stephen M. Kelly[a]

[a] Department of Chemistry, University of Hull, Hull HU6 7RX, UK [b] Department of Chemistry, Northeast Normal University, Changchun, PR China [c] Department of Physics, University of Hull, Hull HU6 7RX, UK

PLEASE SCROLL DOWN FOR ARTICLE

Taylor & Francis
Taylor & Francis Group

Heterocyclic reactive mesogens: synthesis, characterisation and mesomorphic behaviour

MATTHEW P. ALDRED†, PANOS VLACHOS†, DEWEN DONG‡, STUART P. KITNEY†,
W. CHUNG TSOI§, MARY O'NEILL*§ and STEPHEN M. KELLY*†

†Department of Chemistry, University of Hull, Cottingham Rd., Hull HU6 7RX, UK
‡Department of Chemistry, Northeast Normal University, Changchun, PR China
§Department of Physics, University of Hull, Cottingham Rd., Hull HU6 7RX, UK

Novel heterocyclic and photopolymerizable liquid crystalline materials (reactive mesogens) with smectic phases have been synthesized and characterized. A selection of heterocyclic rings, such as benzothiazole, benzothiadiazole and pyrimidine, has been incorporated into the aromatic core to control the electrochemical/luminescence properties and the structural geometry. Particular emphasis is focused on structure–property relationships, in which the variation of molecular structure and its subsequent effect on the liquid crystalline transition temperatures have been investigated.

1. Introduction

In the past decade there has been a great deal of research in academia and industry involving the synthesis of new organic semiconductors along with the evaluation of their physical properties for optoelectronic and electronic applications [1]. At present commercial organic light-emitting devices (OLEDs) use either small aromatic molecules [2] or main chain, conjugated polymers [3, 4] as the charge transport and emission layers. However, the processing costs of OLEDs based on small molecules are high, polymer OLEDs have poor multilayer capability, and low resolution pixellation techniques (shadow masking and printing respectively) are used to process both material types. Consequently there is interest in crosslinked polymer networks to form solution-processable, multi-layer OLEDs. Such OLEDs have the added benefits of photopatternability. Recently a red–green–blue pixellated OLED has been demonstrated based on main chain polyfluorenes with photocrosslinkable oxetane side chains and a photoacid as a cationic initiator [5]. There are a number of other reports describing the photochemical or thermal crosslinking of organic side chain polymers to form insoluble polymer networks as charge–transport and/or emission layers in OLEDs [6–9].

However, the photochemical crosslinking process often caused a substantial degree of photochemical degradation. The photoluminescent properties of a limited number of different kinds of nematic polymer networks and gels have been reported [10–14]. This highlighted the possibility of using light-emitting liquid crystals as polymer networks for use in OLEDs especially with polarised emission. The first OLEDs using liquid crystalline polymer networks formed from polymerisable light-emitting liquid crystals (reactive mesogens, RMs) were reported recently [9, 16, 17]. Such OLEDs appear to have the potential to overcome some of the disadvantages of standard OLEDs. In order to realize this potential new light-emitting liquid crystals for OLEDs are required, which should satisfy a demanding set of criteria: low temperature liquid crystal phases for room temperature processing, a range of molecular energies for electron and hole injection, moderately high charge transport for bright emission, good film forming properties from solution in organic solvents, chemical, photochemical and electrochemical stability, as well as tunable colour and colour purity for multicolour OLEDs.

Only a small number of reactive mesogens for use in OLEDs has been reported so far [16–19]. The large majority of these reactive mesogens are fluorene derivatives and exhibit a nematic phase [16–18, 20–23]. Steric effects exerted by the two alkyl chains at the 9-position prevent formation of the layer structure of smectic phases. The lower viscosity of the nematic phase

*Corresponding author. Email: s.m.kelly@hull.ac.uk and m.oneill@hull.ac.uk

compared with that of the smectic phase allows them to be spontaneously aligned on a suitable surface for polarized emission [16]. Liquid crystals also exhibit efficient charge-transporting properties due to the high degree of molecular order and self-organization present in the liquid crystalline state [19]. High charge-mobility has been reported within the smectic phase of various liquid crystalline materials [24–26] and more recently in the nematic phase of a light-emitting fluorene-based reactive mesogen $(1 \times 10^{-3}\,\mathrm{cm^2\,v^{-1}\,s^{-1}})$ [18]. However, smectic reactive mesogens may exhibit better charge transport properties than the corresponding nematic reactive mesogens, due to the higher degree of internal order resulting from the presence of a layered structure, greater overlap of the molecular orbitals responsible for charge transport and a shorter intermolecular distance due to the absence of the alkyl chains acting as lateral substituents in fluorene derivatives.

It has been reported that the crosslinking of reactive mesogens can also result in an increase of the charge carrier mobility by a factor of two [20]. Acrylate, methacrylate and non-conjugated diene groups, which polymerize by a radical mechanism, are preferred as photochemically-initiated polymerizable end groups, rather than vinyl ethers, epoxides or oxetanes, for example, which require ionic initiators or chemical crosslinking agents such as amines in the case of epoxides. Such initiators remain within the highly crosslinked polymer networks and are suspected of causing short device lifetimes. Non-conjugated diene groups exhibit a combination of favourable properties such as (i) thermal stability at moderately high temperatures, (ii) tendency to lower the melting points of liquid crystals and (iii) the ability to form highly insoluble crosslinked networks. In some unusual cases a photoinitiator is not required to initiate the crosslinking reaction. Smectic liquid crystals often incorporate heterocyclic rings in the central aromatic core. Therefore, in this paper, we report the synthesis and characterization of novel heterocyclic light-emitting and charge-transporting smectic reactive mesogens without a fluorene moiety and with acrylate, methacrylate and non-conjugated diene end groups.

2. Results and discussion

With respect to OLEDs hole-injection materials with low ionization potentials (IPs) and electron-injection materials with high electron affinities (EAs) are required. The standard strategy to increase/decrease the IP of a molecule is to include an electron with-drawing/donating group in its aromatic core or by incorporating adjacent electron-deficient/electron-rich atoms. Most conjugated organic materials are electron
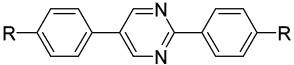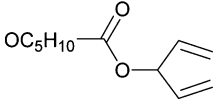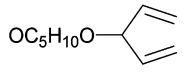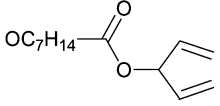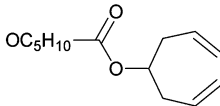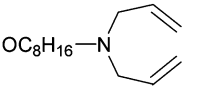
rich, therefore it is not surprising that in many cases these materials transport holes (cationic radicals), rather than electrons (anionic radicals). Enhancing the electron affinity of a molecule can be achieved by incorporating electron-deficient nitrogen atoms in the molecular structure. This can be achieved by synthesizing materials that include heterocyclic aromatic rings such as oxadiazole [27], triazole [27–29], and quinoxaline [30]. In this paper, we report the incorporation of nitrogen-containing heterocycles, such as pyridine, pyrimidine and tetrazine, and the incorporation of nitrogen and sulphur(oxygen)-containing heterocycles, such as benzothiazoles and benzothia(oxa)diazoles. The molecular structures were kept as simple as possible because in general the overlap of molecular wavefunctions is often more important than the structure itself [31]. OLED fabrication and measurements, such as charge-carrier mobility and electroluminescence have been carried out on most of these compounds and the physical data is described elsewhere [32].

2.1. Pyridine, pyrimidine and tetrazine

Charge-transporting reactive mesogens that incorporate a central pyrimidine heterocyclic ring are shown below, in which diene, acrylate, methacrylate and diallylamine moieties are used as the photoreactive groups attached via spacers to both ends of the aromatic core. Table 1 shows the effect of changing the type of the polymerizable end group and varying the spacer length (number of methylene units) on the liqui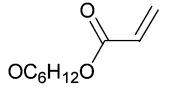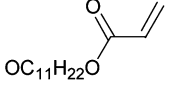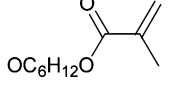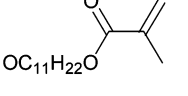d crystalline transition temperatures. It has been demonstrated that the melting point can be lowered significantly when the number of methylene groups in the spacer is increased [18]. **PYM-1** is the first charge-transporting room temperature smectic liquid crystal and shows relatively high electron-transport properties $(1.5 \times 10^{-5}\,\mathrm{cm^2\,v^{-1}\,s^{-1}})$ [26]. The low melting point allows device fabrication to be carried out at room temperature, when **PYM-1** is used as a charge-transporting layer.

2.1.1. Synthesis. The synthesis of the pyrimidine- and tetrazine-based compounds are outlined in schemes 1 and 2 respectively. The analogous pyridine-based liquid crystal was synthesized in the same manner outlined in scheme 1; however, dibromopyridine was used in the Suzuki cross-coupling reaction, as opposed to bromochloropyrimidine. Scheme 1: alkylation [33] of 4-bromophenol (**1a**) with (*S*)-citronellyl bromide and subsequent boronic acid formation [34] produced the phenyl boronic acid (**1c**). Citronellyl bromide was chosen as the terminal group of this and the following reaction intermediates as it induces high solubility in common organic solvents due to the branching methyl

Table 1. Transition temperatures (°C) of **PYM** compounds.

Compound	R	Cr		SmC		I
PYM-1	OC$_5$H$_{10}$ ...	•	25	•	124	•
PYM-2	OC$_5$H$_{10}$O ...	•	58	•	175	•
PYM-3	OC$_7$H$_{14}$ ...	•	56	•	126	•
PYM-4	OC$_5$H$_{10}$ ...	•	73	•	108	•
PYM-5	OC$_8$H$_{16}$—N ...	•	52	•	116	•
PYM-6	OC$_6$H$_{12}$O ...	•	78	•	123	•
PYM-7	OC$_{11}$H$_{22}$O ...	•	82	•	150	•
PYM-8	OC$_6$H$_{12}$O ...	•	55	•	123	•
PYM-9	OC$_{11}$H$_{22}$O ...	•	97	•	141	•

Scheme 1.   Reagents and conditions: (i) K_2CO_3, (*S*)-citronel-lyl bromide, butanone, reflux , (ii) (a) *n*-BuLi, THF, $-78^\circ C$, (b) $B(OMe)_3$ (c) H_3O^+ (iii) Na_2CO_3 (2M) , $Pd(PPh_3)_4$, DME, $100^\circ C$ (iv) (a) BBr_3, CH_2Cl_2, (b) H_2O (ice) (v) RBr, K_2CO_3, DMF, $90^\circ C$.

groups. Aryl–aryl Suzuki cross-coupling [35] of bromochloropyrimidine and the phenyl boronic acid (**1c**) produced the diether (**1d**) with three aromatic rings in the core. Deprotection of **1d**, using boron tribromide [36], afforded the bis-phenol **1e**, which was alkylated using the bromo-substituted diene-esters/acrylates and methacrylates in a Williamson ether synthesis to give the desired compounds (**PYM-1** to **PYM-9**). The bromo-substituted diene-ester, 1,4-pentadien-3-yl 6-bromohexanoate, was synthesized by base-assisted esterification [37] using the commercially available secondary alcohol, 1,4-pentadien-3-ol, and the commercially available 6-bromohexanoyl chloride. The
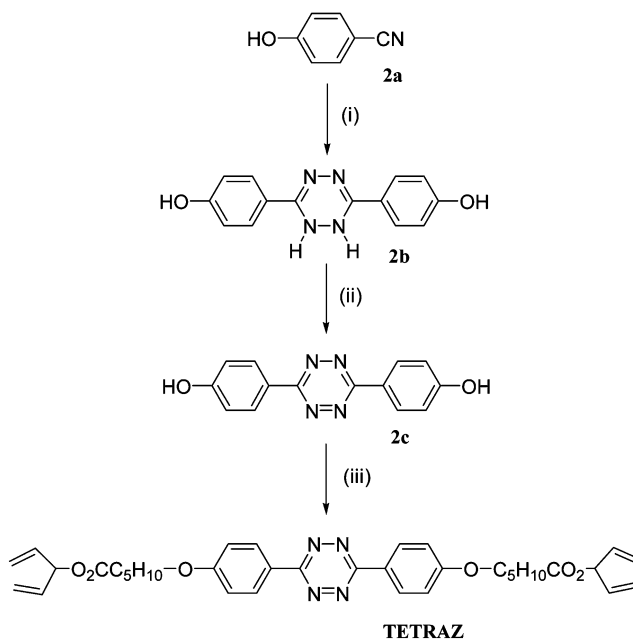
Scheme 2.   Reagents and conditions: (i) hydrazine hydrate, reflux, (ii) acetic acid:water (2:1), sodium nitrite, (iii) 1,4-pentadien-3-yl 6-bromohexanoate, K_2CO_3, DMF, $90^\circ C$.

longer chain bromoester-dienes, viz. 1,4-pentadien-3-yl 11-bromoundecanoate, were synthesized by esterification of the corresponding commercially available bromoalkanoic acids using DCC, DMAP and 1,4-pentadien-3-ol [38]. Bromo-substituted acrylate and methacrylate alkylating reagents were synthesized by the esterification of the respective bromoalkanol with acryloyl or methacroyl chloride. Scheme 2: 4-hydroxybenzonitrile (**2a**) was purchased from Aldrich and was used without further purification. Heating compound **2a** under reflux with hydrazine hydrate and subsequent oxidation of compound **2b** using sodium nitrite [39] afforded the tetrazine bis-phenol **2c** [40]. The bis-phenol was alkylated, using the appropriate bromo-substituted diene-ester, in a Williamson-ether synthesis to give the desired compounds (**TETRAZ-1** and **TETRAZ-2)**.

2.1.2. Mesomorphic properties. All the reactive mesogens **PYM-1** to **PYM-9** exhibit an enantiotropic smectic C phase, see figure 1, with relatively high clearing points (SmC–I). All the pyrimidines **PYM-1** to **PYM-5** show optical textures characteristic of a SmC phase. Schlieren texture with 4-brush disclinations is observed in the liquid crystal phase and no droplets are seen on cooling slowly from the isotropic phase into the liquid crystalline phase. No 2-brush disclinations are observed either. Surprisingly, the melting point and clearing point are observed to increase when the spacer
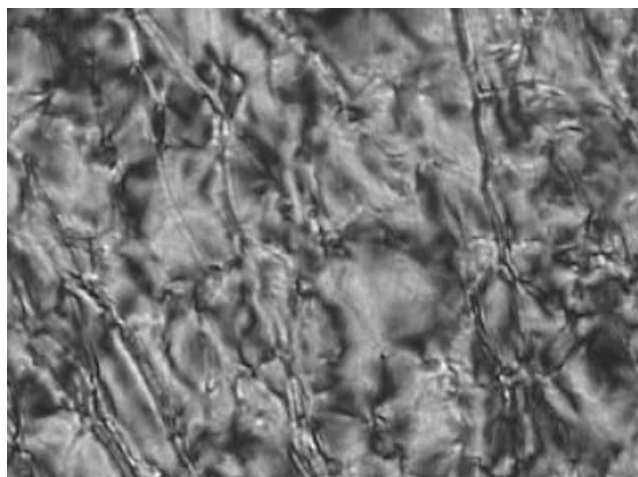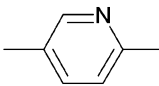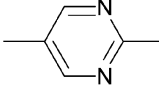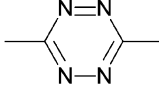
Figure 1. Schlieren texture of the SmC phase of **PYM-1** at room temperature.

length is increased (**PYM-1** and **PYM-3**). Compound **PYM-2**, contains an ether-diene polymerizable group, rather than the analogous ester-diene group. However, this modification of the polymerizable group leads to a higher melting point. This may be due to the more linear character of the ether-diene end group compared with the ester-diene end group. The presence of other polymerizable groups, such as 1,6-octadiene (**PYM-4**) and diallylamine (**PYM-5**) also leads to a high melting point. Therefore, the 1,4-pentadiene appears to be the most effective of the diene polymerizable groups with

respect to melting point. It is also the fastest polymerizable diene end group due to the presence of fewer allylic hydrogen atoms, which consequently improves the degree of polymerisation [41]. Therefore, in the remainder of this paper, the 1,4-pentadiene group is incorporated as the photoreactive end group in all the reactive mesogens. The acrylates (**PYM-6** and **PYM-7**) exhibit similar transition temperatures to those of the dienes (**PYM-1** to **PYM-5**). The transition temperatures of the methacrylates (**PYM-8** and **PYM-9**) are lower than those of the corresponding acrylates (**PYM-6** and **PYM-7**) due to the steric effect of the methyl group. The molecular structures shown in table 2 differ by the number of nitrogen atoms present in the central aromatic ring.

The pyridine **PYR-1** with one nitrogen atom in the central ring possess a similar clearing point to that of the corresponding pyrimidine **PYM-1** with an otherwise identical structure apart from the replacement of another C-H unit by a nitrogen atom. However, the melting point is much higher, which leads to a much narrower mesophase temperature range for the pyridine. The tetrazine **TETRAZ-1** with four nitrogen atoms in the central ring exhibits an even higher melting point than those of **PYM-1** and **PYR-1**. This difference can be attributed to the different packing of the molecules in the crystalline state. **PYM-1** has two ring junctions between a pyrimidine ring and a phenyl ring. The asymmetry present in the pyrimidine ring results in

Table 2. Transition temperatures (°C) with varied N atom numbers.

Compound		Cr		SmC		I
PYR-1		•	87	•	126	•
PYM-1		•	25	•	124	•
TETRAZ-1		•	109		—	•

two unequal dihedral angles. Molecular modelling, using CS Chem3D Pro, confirms that one half of the molecule can be viewed as being similar to a biphenyl unit with significant inter-annular twisting (~40°). No significant inter-annular twisting (~0–1°) is present in the other half of the molecule because the atoms *ortho* to the ring junction are not constrained away from each other. **TETRAZ-1** is an almost planar molecule because the atoms *ortho* to the ring junction are not forced away from each other and hence there is no significant twist between the aromatic units. Modelling shows that the two dihedral angles are equal and approximately 0–1°. Therefore, it can be supposed that the smaller the dihedral angle, the greater the degree of polarizability between the π-systems of each aromatic ring. This gives rise to more efficient packing of the molecules and consequently higher melting points. The planar nature of **TETRAZ-1** makes it a promising candidate for a charge-transporting material due to the potential for greater overlap of the π in a π–π stacking arrangement. **TETRAZ-1** does not exhibit an observable mesophase, possibly due to the high melting point, although it may exhibit a monotropic-phase. However, by increasing the methylene units between the tetrazine-containing aromatic core and the diene end-groups, from 5 to 10, a liquid crystalline phase is observed, see figure 2 (**TETRAZ-2**, Cr 80 SmC 132 I). This may be due to the lowering of the melting point, which allows the mesophase to become apparent.

2.2. *Benzothiazoles*

Some liquid crystalline materials incorporating a benzothiazole-fused ring structure in the molecular core exhibit good hole-transporting properties with a low
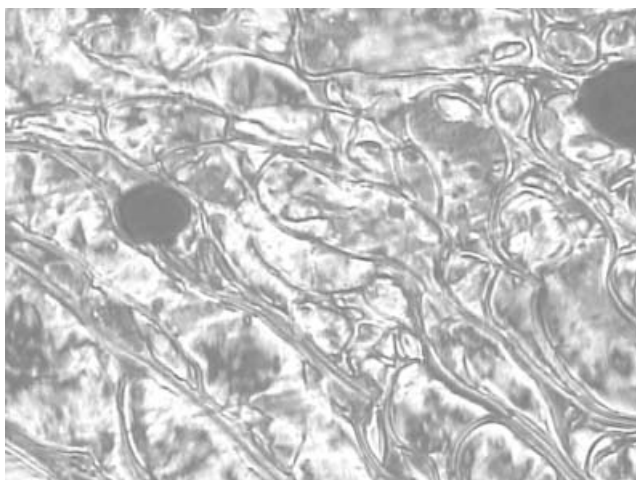

Figure 2. Schlieren texture of the SmC phase of **TETRAZ-2** at 125°C.

ionization potential, which makes them of potential interest as hole-transporting materials in OLEDs [42–44]. However, the liquid crystalline benzothiazoles for which transport properties have been reported are crystalline at room temperature; they are not polymerizable and are therefore unusuable in multi-layer OLED devices. Therefore, the benzothiazole reactive mesogens shown in table 3 were synthesized. The molecular structure was varied to investigate the dependence of the liquid crystalline transition temperatures and mesophase behaviour on the molecular structure.

2.2.1. Synthesis. This was carried out as indicated in schemes 3 and 4. Scheme 3: the aminothiols **3a** and **3b** were synthesized by base-hydrolysis of commercially available 2-amino-6-ethoxybenzothiazole and 5-methoxy-2-methylbenzothiazole, respectively, according to the literature [45]. The benzaldehyde **3c** was prepared by a Williamson ether reaction of 4-hydroxybenzaldehyde and 8-bromooctane using K_2CO_3. Condensation of the benzaldehyde **3c** and the aminothiols **3a** and **3b**, in DMSO [46], produced the benzothiazoles **3d** and **3e**. Deprotection, using boron tribromide, produced the assymetric bis-phenols **3f** and **3g**. Williamson ether synthesis of compounds **3f** and **3g** with the appropriate bromo-substituted diene-esters afforded the final products **BTHAZ-1** to **BTHAZ-4**. Scheme 4: the branched chain was synthesised from the commercially available (*S*)-(+)-citronellyl bromide. Epoxidation [47] of (*S*)-(+)-citronellyl bromide (**4a**) using *m*-chloroperbenzoic acid, produced the corresponding epoxide (**4b**). Oxidative cleavage [49] of the epoxide with periodic acid in tetrahydrofuran and quenching with water produced the aldehyde (**4c**). A 'one-pot' procedure to obtain the carboxylic acid was attempted by direct oxidation of (*S*)-(+)-citronellyl bromide, using potassium permangenate and 18-crown-6 in benzene [49, 50] (so called 'purple benzene'). However the yield was very low and

Table 3. Transition temperatures (°C) of **BTHAZ** compounds (**1**–**4**).

Compound	*m*	Cr		SmC		I
BTHAZ-1	2,5–	5	•	40	(• −23)	•
BTHAZ-2	2,6–	5	•	63	(• 39)	•
BTHAZ-3	2,6–	7	•	55	• 64	•
BTHAZ-4	2,6–	10	•	49	• 71	•
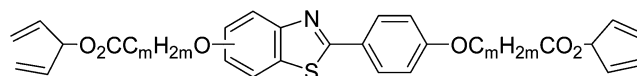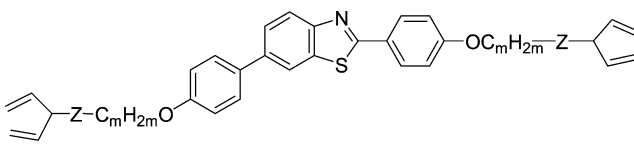
Table 4. Transition temperatures ($^{\circ}$C) of **BTHAZ** compounds (**6–10**).

Compound	Z	m	Cr		SmC		N		I
BTHAZ-6	CO_2	5	•	82		—	•	147	•
BTHAZ-7	CO_2	10	•	68		—	•	187	•
BTHAZ-8	O	5	•	104	•	171		—	•
BTHAZ-9	O	6	•	95	•	165		—	•
BTHAZ-10	O	8	•	89	•	150		—	•

purification of the carboxylic acid was difficult. The aldehyde was oxidised using Jones reagent [51] in acetone to produce the carboxylic acid (**4d**), which was esterified using DCC, DMAP and 1,4-pentadien-3-ol to produce the diene-ester (**4e**). The final product **BTHAZ-5** was prepared by a Williamson alkylation in
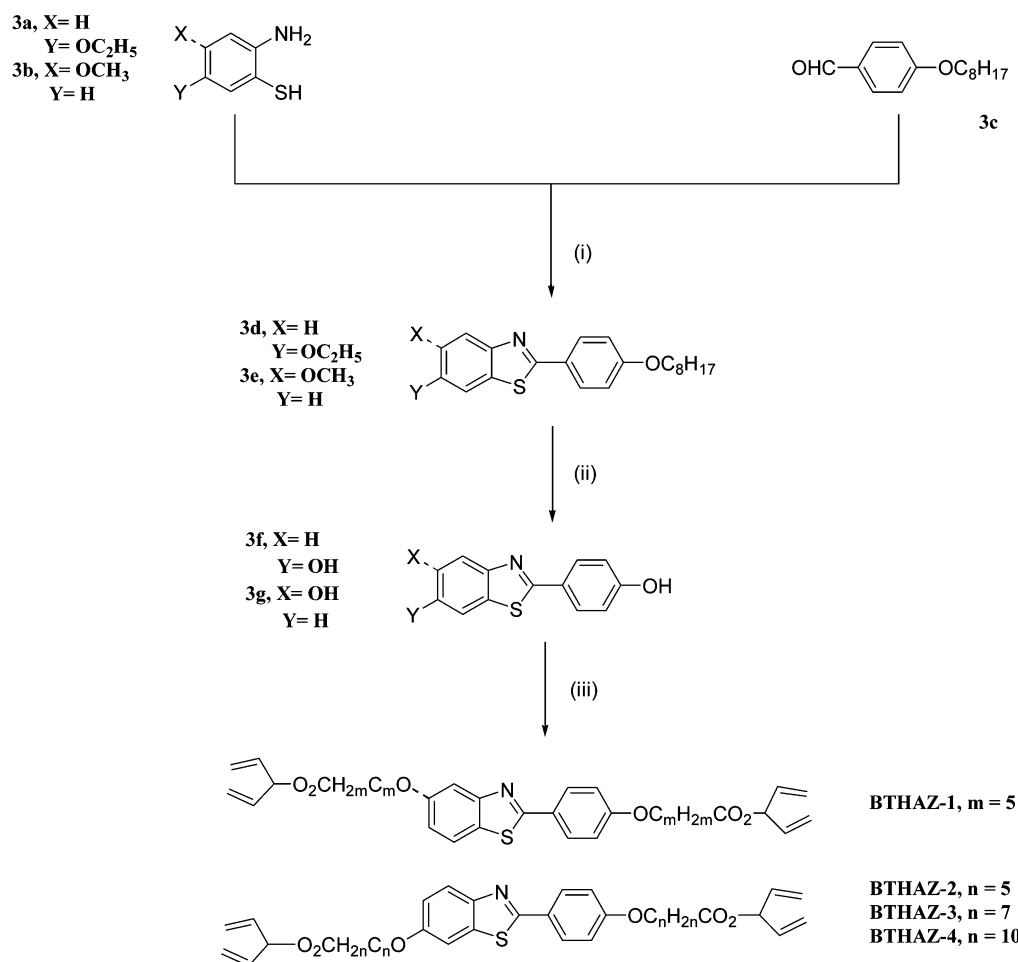
Scheme 3. Reagents and conditions: (i) DMSO, 90°C, (ii) (a) BBr$_3$, CH$_2$Cl$_2$, (b) H$_2$O (ice), (iii) 1,4-pentadien-3-yl 6-bromohexanoate (**BTHAZ-1** and **BTHAZ-2**), 1,4-pentadien-3-yl 8-bromooctanoate (**BTHAZ-3**), 1,4-pentadien-3-yl 11-bromoundecanoate (**BTHAZ-4**), K$_2$CO$_3$, DMF, 90°C.
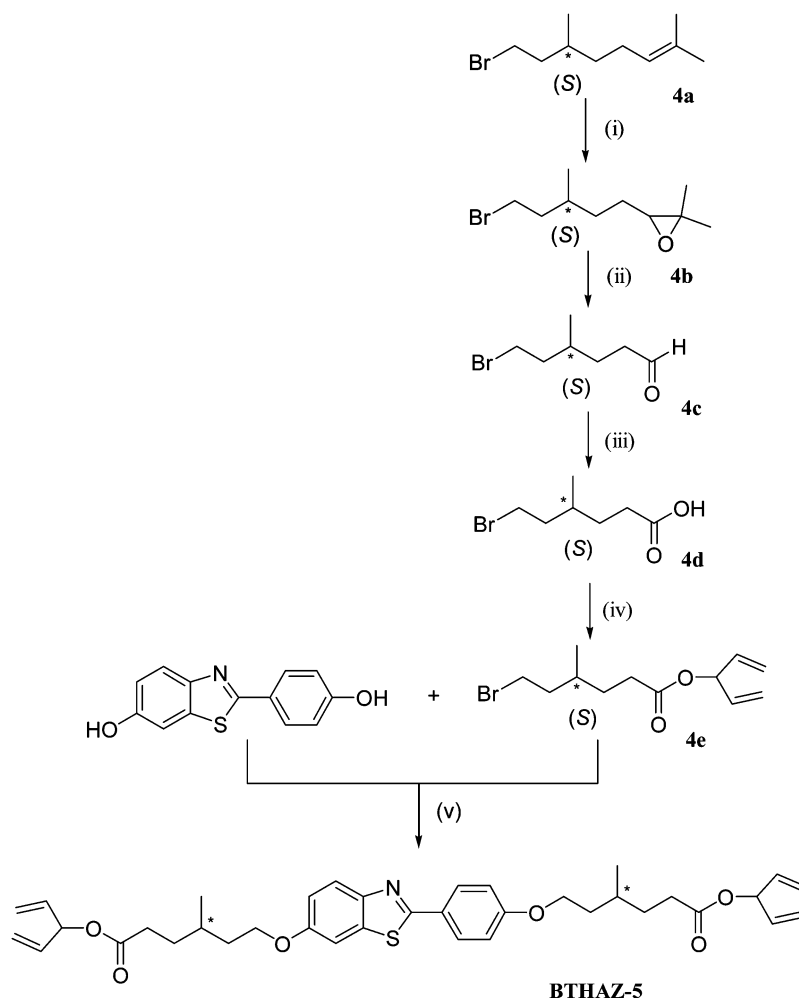
Scheme 4. Reagents and conditions: (i) *m*-chloroperbenzoic acid, CH$_2$Cl$_2$, (ii) (a) periodic acid, THF, (b) H$_2$O, (iii) (a) Jones reagent, acetone, (b) propan-2-ol, (iv) DCC, DMAP, CH$_2$Cl$_2$, (v) *R*Br, K$_2$CO$_3$, DMF, 90°C

the normal way using the bromo-substituted diene-ester (**4e**) and the phenol (**3f**).

2.2.2. Mesomorphic behaviour.

The position of the spacer and polymerizable end group at either the 5- or 6-position of the phenyl ring of the benzothiazole core has a significant effect on mesomorphic behaviour (see tables 3 and 4). The non-colinear 2,5-disubstitution pattern of the benzothiazole unit is not particularly favourable (figure 3) for mesophase formation and accordingly **BTHAZ-1** exhibits a monotropic mesophase below 0°C. The 2,6-disubstituted benzothiazole (figure 4) has a more linear molecular structure compared to that of the analogous 2,5-disubstituted benzothiazole with the same substituents and, therefore, the 2,6-disubstituted benzothiazoles (**BTHAZ-2** to **BTHAZ-4**) exhibit much higher clearing points than those of the corresponding 2,5-disubstituted benzothiazoles. The greater degree of flexibility of the

alkyl spacers between the aromatic core and the photopolymerizable diene end group of the benzothiazoles (**BTHAZ-3** and **BTHAZ-4**) with longer chains ($n=7$, 10) is probably responsible for the lower melting points of these homologues compared with **BTHAZ-2**. This may be due to the presence of more non-linear chain conformations, which in turn leads to a lower degree of anisotropy of molecular shape and polarizability. In contrast, the clearing point increases with increasing number of methylene units in the spacer as is sometimes observed. The presence of a branching methyl group in the spacer between the aromatic core and the polymerizable end group in **BTHAZ-5** leads to a lower melting point (Cr 53 SmC* 62 I) compared with that of the corresponding **BTHAZ-2** with the same spacer length. This is due to steric effects related to the bulky methyl group. In addition, the chiral centre induces a chiral smectic C phase.
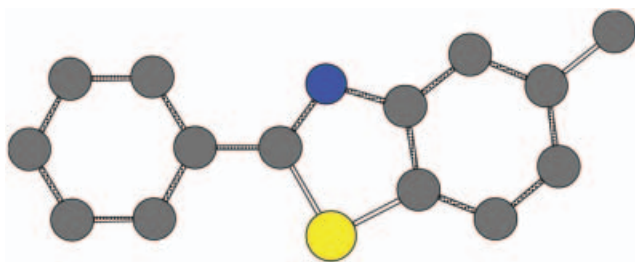
Figure 3.   2,5-Disubstituted benzothiazole.

The presence of an additional phenyl ring in the 2,6-disubstituted benzothiazoles (**BTHAZ-6** to **BTHAZ-10**) compared with those of the 2,6-disubstituted benzothiazoles (**BTHAZ-2** to **BTHAZ-4**) shown in table 3 leads to higher melting points and clearing points as expected due to a greater length-to-breadth ratio. The esters (**BTHAZ-6** and **BTHAZ-7**) exhibit a nematic phase whereas the ethers (**BTHAZ-7** to **BTHAZ-9**) possess a smectic C phase.

2.3.   *Benzothiadiazoles and Benzoxadiazoles*

Main chain conjugated polymers incorporating 4,7-disubstituted benzothiadiazoles have been shown to possess excellent charge-transport and electroluminescent properties [52, 53]. Therefore, reactive mesogens incorporating a 4,7-disubstituted benzothiadiazole were synthesized. The synthesis of an analogous reactive mesogen incorporating a 2,7-disubstituted benzoxadiazole was also carried out in order to investigate the replacement of a sulphur heteroatom with an oxygen heteroatom, contained in the central heterocyclic ring, and its affect on the liquid crystalline transition temperatures and other properties; see later.

2.3.1.   Synthesis.
Protection of 4-bromophenol **5e** was achieved using 3,4-dihydro-2*H*-pyran to afford the corresponding THP ether **5f**, which was converted to the corresponding boronic ester **5g** according by literature methods [54]; see scheme 5. Compounds **5c** and **5d** were synthesized by the bromination of commercially available benzothiadiazole and benzooxadiazole (**5a** and **5b**, respectively), using
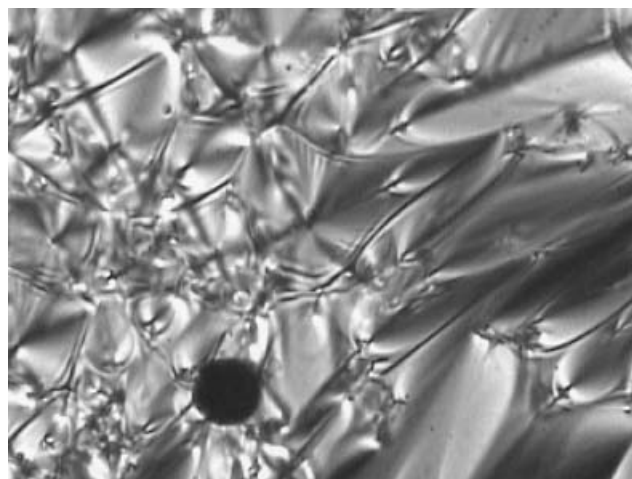

Figure 4.   2,6-Disubstituted benzothiazole.

Figure 5.   The focal conic fan-like texture of the SmA phase of **BTDAZ-1** at 75 °C.

HBr$_{aq}$ (48%) and bromine [55]. Suzuki aryl–aryl cross coupling of compounds **5c/5d** and **5g** using *tetrakis*(triphenylphosphine)palladium(0) in anhydrous conditions produced compounds **5h/5i**. Deprotection using *para*toluenesulphonic acid (PTSA) in dichloromethane/ethanol yielded the corresponding bis-phenols, which were alkylated in a Williamson ether reaction to yield the novel reactive mesogens (**BTDAZ-1**, **BTDAZ-2** and **BODAZ**).

2.3.2.   Mesomorphic properties.
The benzoxadiazole (**BODAZ-1**) exhibits a higher clearing point and a lower melting point than the corresponding benzothiadiazole (**BTDAZ-1**), see table 5. Consequently, the temperature range of the smectic A phase, see figure 5, is much broader. The liquid crystal transition temperatures of the homologues (**BTDAZ-1** to **BTDAZ-3**) decrease with increasing chain length. This can be explained by the presence of more non-linear conformations of the terminal chains. The presence of a fluorine atom in the benzothiadiazole (**BTDAZ-4**) in place of the hydrogen atom in the same position in the analogous compound benzothiadiazole (**BTDAZ-2**) leads to lower transition temperatures due to steric effects. However, the clearing point is decreased more than the melting point and so the smectic A phase is monotropic.

3.   Electrochemical properties

The ionization potentials (IPs) of the reactive mesogens were measured electrochemically by CV using a computer-controlled scanning potentiostat (Solartron 1285). 1 mM of the compound was dissolved in 5 cm^3 of an electrolytic solution of 0.3 M tetrabutylammonium
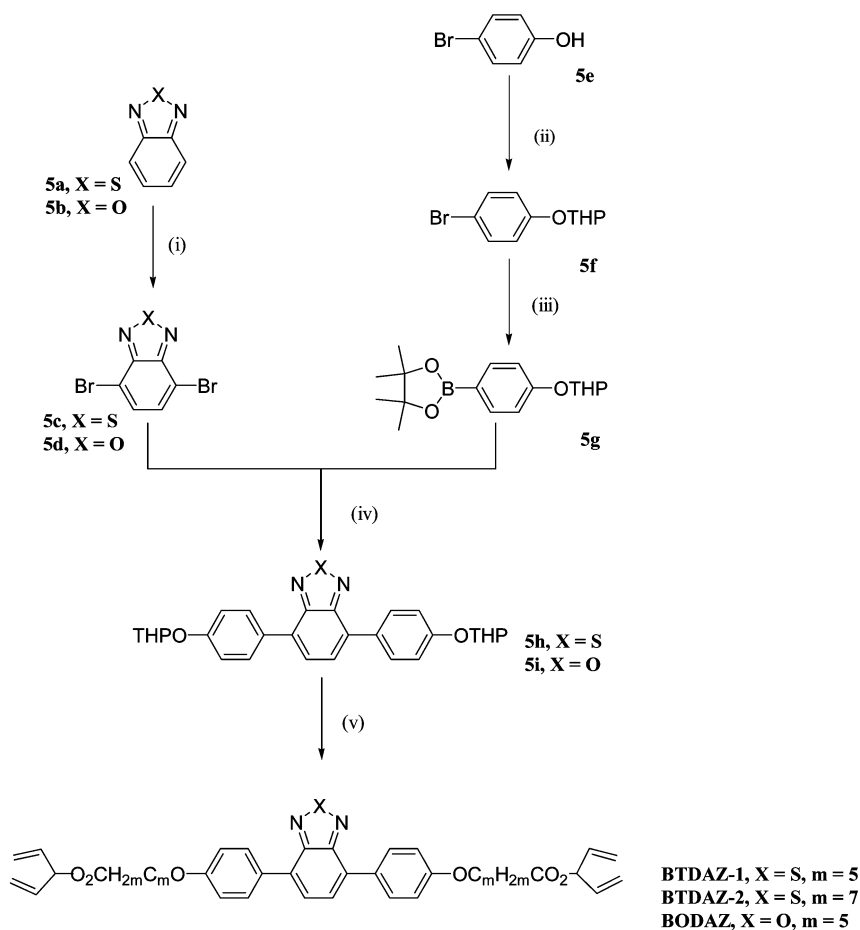
Scheme 5. Reagents and conditions: (i) HBr$_{(aq)}$, Br$_2$, (ii) DHP, PTSA, DCM, (iii) (a) *n*-BuLi, THF, −78°C, (b) (ii) 2-isopropoxy-4,4,5,5-tetramethyl-1,3,2-dioxaborolane (iv) K$_3$PO$_4$, Pd(PPh$_3$)$_4$, DMF, 90°C, (v) PTSA, EtOH.DCM, 1,4-pentadien-3-yl 6-bromohexanoate (**BTDAZ-1** and **BODAZ**), 1,4-pentadien-3-yl 8-bromooctanoate (**BTDAZ-2**), K$_2$CO$_3$, DMF, 90°C.

hexafluorophosphate in dichloromethane. The solution was placed in a standard three-electrode electrochemical cell. A glassy carbon electrode was used as the working electrode. Silver/silver chloride (3M NaCl and saturated AgCl) and a platinum wire formed the reference and counter electrodes respectively. The electrolyte was recrystallized twice before use and oxygen contamination was avoided by purging the solution with dry argon

Table 5. Transition temperatures (°C) of **BODAZ** and **BTDAZ** compounds.
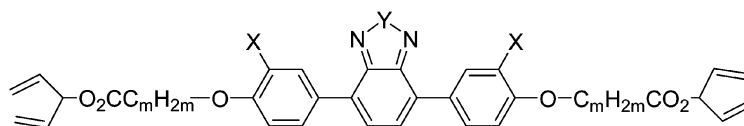
Compound	X	Y	m	Cr		SmA		I
BODAZ-1	H	O	5	•	60	•	98	•
BTDAZ-1	H	S	5	•	69	•	84	•
BTDAZ-2	H	S	7	•	57	•	73	•
BTDAZ-3	H	S	10	•	64	•	77	•
BTDAZ-4	F	S	10	•	54	(•	48)	•

before each measurement. The measured potentials were corrected to an internal ferrocene reference added at the end of each measurement. A typical scan rate of $20\,mV\,s^{-1}$ was used; two scans were performed to check the reproducibility. We were unable to measure a value for the reduction potential because of the limited working range of the electrolyte and solvent. However electron affinity (EA) was estimated by subtraction of the optical band-edge, taken as the energy of the onset of absorption of the compound, from the IP. The electron affinities of **BTDAZ-1** and **BODAZ-1** are closely matched to the work-function of calcium $(=2.8\,eV)$ so they may be suitable as electron-injection layers in a multilayer organic light-emitting device. **PYR-1** and **PYM-1** are not particularly suitable for electron injection from Ca nor hole injection from InSnO (workfunction $4.8\,eV$) because of the high barriers. **TETRAZ-1** may provide a good electron-accepting hole blocking layer in an organic solar cell because of its high IP, EA and small E_g. Electrochemical results are collected in table 6.

4. Experimental

Schemes 1–5 illustrate the synthetic pathways used in the synthsesis of our novel reactive mesogens. Selected syntheses are given below, in which the synthesis for **BTHAZ-2** to **BTHAZ-5** (scheme 3 and scheme 4) is represented. All commercially available starting materials, reagents and solvents were used as supplied and were obtained from Aldrich, Strem Chem. Inc., Acros or Lancaster Synthesis. All reactions were carried out using a dry nitrogen atmosphere unless water was present as solvent or reagent and the temperatures were measured internally. Mass spectra were recorded using a Gas Chromatography/Mass Spectrometer (GC/MS)-QP5050A Schimadzu with Electron Impact (EI) at a source temperature of 200°C. IR spectra were recorded using a Perkin-Elmer Paragon 1000 Fourier Transform-Infrared (FTIR) spectrometer. ^1H NMR spectra were recorded using a JEOL Lambda 400 spectrometer and

an internal standard of tetramethylsilane (TMS) was used. GC was carried out using a Chromopack CP3800 gas chromatogaph equipped with a $10\,m$ CP-SIL 5CB column. Purification of intermediates and final products was accomplished mainly by gravity column chromatography [1], using silica gel (40–63 microns, $60\,A$) obtained from Fluorochem. The melting point and liquid crystal transition temperatures of the solids prepared were measured using a Linkam 350 hot stage and control unit in conjunction with a Nikon E400 polarizing microscope. The transition temperatures of all the final products were confirmed using a Perkin-Elmer DSC-7 in conjunction with a TAC 7/3 instrument controller, using the peak measurement for the reported value of the transition temperatures. The purity of all final compounds was checked by elemental analysis using a Fisons EA 1108 CHN analyzer.

4.1. *2-Amino-5-ethoxybenzothiol (3a)*

A solution of potassium hydroxide $(500\,g)$ in water $(400\,cm^3)$ was added carefully to a suspension of 2-amino-6-ethoxybenzothiazole and ethanol $(400\,cm^3)$. The reaction mixture was heated under reflux for 72 h, cooled to r.t. and filtered. The filtrate was acidified with acetic acid until it became slightly acidic. The excess acetic acid was evaporated under reduced pressure and water was added $(500\,cm^3)$. The product was extracted into diethyl ether $(2 \times 300\,cm^3)$, washed with water $(2 \times 200\,cm^3)$, dried $(MgSO_4)$, filtered and concentrated under reduced pressure to yield a light green powder (6.15 g, 14.1%). The product was used without further purification. M.p./°C: 92–94 (Lit. 104 [38]); Purity: $\sim$90% (NMR); ^1H NMR $(CDCl_3)$ δ_H: 1.31 (3H, t), 3.80 (2H, quart), 6.67 (1H, d, $J=8.7\,Hz$), 6.72 (1H, d, $J=2.8\,Hz$), 6.79 (1H, dd, $J=3.1, 8.7\,Hz$), $-NH_2$ and $-SH$ not detected; IR v_{max}/cm^{-1}: 3386, 3282, 3183, 3045, 2979, 2933, 2889, 1659, 1623, 1589, 1495, 1406, 1328, 1229, 1115, 1051, 939, 858, 823; MS m/z (EI): 169 (M$^+$, M100), 168, 140, 122, 112, 96, 78, 67.

Table 6. Electrochemical results.

Compound	X^1	X^2	X^3	X^4	IP^a/eV ± 0.02	$E_g{}^b$/eV ± 0.04	EA^c/eV ± 0.06	Remark
PYR-1	N	C	C	C	5.40	3.33	2.07	Irreversible
PYM-1	N	N	C	C	5.57	3.42	2.15	Irreversible
TETRAZ-1	N	N	N	N	5.64	2.06	3.58	Reversible
BTHAZ-4	—	—	—	—	5.41	3.38	2.03	Reversible
BTDAZ-1	—	—	—	—	5.34	2.65	2.69	Reversible
BODAZ-1	—	—	—	—	5.42	2.55	2.87	Reversible

4.2. 6-Ethoxy-2-(4-octyloxyphenyl)benzothiazole (3d)

A solution of 4-octyloxybenzaldehyde (**3c**) (2.90 g, 0.0124 mol), Compound **3a** (2.30 g, 0.0136 mol) and DMSO (40 cm^3) was heated at 90°C for 48 h. The cooled solution was added to water (200 cm^3) and extracted into diethyl ether (200 cm^3). The aqueous layer was washed with diethyl ether (2 × 150 cm^3) and the combined ethereal extracts washed with brine (3 × 100 cm^3), dried (MgSO$_4$), filtered and concentrated under reduced pressure. The residue was purified by gravity column chromatography (silica gel, DCM/hexane, 80/20%) and recrystallised from ethanol to yield a white powder (2.32 g, 48.7%). Transition temp. /°C: Cr 106 SmC 134 I.; ^{1}H NMR (CDCl$_3$) δ_H: 0.89 (3H, t), 1.24–1.41 (8H, m), 1.46 (3H, t), 1.46–1.51 (2H, m), 1.81 (2H, quint), 4.02 (2H, t), 4.10 (2H, quart), 6.96 (2H, d, *J*=8.7 Hz), 7.05 (1H, dd, *J*=2.5, 9.0 Hz), 7.32 (1H, d, *J*=2.5 Hz), 7.89 (1H, d, *J*=8.7 Hz), 7.96 (2H, d, *J*=8.7 Hz); IR ν_{max}/cm^{-1}: 3066, 2951, 2924, 2858, 1604, 1523, 1457, 1222, 1169, 1027, 965, 937, 830, 692; MS (*m/z*) (EI): 383 (M$^+$, M100), 356, 271, 242, 214, 180, 152, 122, 107, 95, 77, 69; Elemental analysis, expected: C 72.02, H 7.62, N 3.65, S 8.36; obtained: C 72.27, H 7.85, N 3.53, S 8.62%.

4.3. 2-(4-Hydroxyphenyl)-6-hydroxybenzothiazole (3f)

Boron tribromide (1.90 cm^3, 0.0201 mol) in DCM (15 cm^3) was added dropwise to a cooled (0°C) stirred solution of comopound (**3d**) (2.20 g, 0.0057 mol) in DCM (80 cm^3). The reaction mixture was stirred at r.t. overnight, then poured onto an ice/water mixture (200 g) and stirred for 30 min. The product was extracted into ethyl acetate (2 × 100 cm^3). The combined organic layers were washed with water (100 cm^3), dried (MgSO$_4$), filtered and concentrated under reduced pressure. DCM (50 cm^3) was added and the product filtered. The crude product was purified by washing with hot DCM (2 × 20 cm^3) and filtering to yield a light yellow powder (1.20 g, 86.3%). M.p./°C: 256; ^{1}H NMR (CDCl$_3$) δ_H: 6.89 (2H, d, *J*=8.7 Hz), 6.94 (1H, dd, *J*=2.5, 9.0 Hz), 7.35 (1H, d, *J*=2.5 Hz), 7.76 (1H, d, *J*=8.7 Hz), 7.84 (2H, d, *J*=8.7 Hz), 9.80 (1H, s, –OH), 10.10 (1H, s, –OH); IR ν_{max}/cm^{-1}: 3200–3400, 3050, 1605, 1580, 1490, 1454, 1261, 1227, 1179, 1059, 980, 829; MS (*m/z*) (EI): 243 (M$^+$, M100), 214, 213, 170, 119, 95, 85, 69.

4.4. 6-[5-(1-Vinylallyloxycarbonyl)pentyloxy]-2-{4-[5-(1-vinylallyloxycarbonyl)pentyloxy]phenyl}benzothiazole (BTHAZ-2)

A mixture of compound **3f** (0.10 g, 4.12 × 10^{-4} mol), 1,4-pentadien-3-yl 6-bromohexanoate (0.81 g,

9.47 × 10^{-4} mol) and potassium carbonate (0.17 g, 0.0012 mol) in DMF (5 cm^3) was heated at 90°C for 48 h. The reaction mixture was cooled to r.t., water (50 cm^3) was added and the product extracted into DCM (2 × 100 cm^3). The combined organic layers were washed with brine (4 × 100 cm^3), dried (MgSO$_4$), filtered and concentrated under reduced pressure. The crude product was purified by gravity column chromatography (silica gel, ethyl acetate/hexane, 20/80%) to yield a white solid (0.10 g, 40%). Transition temp. /°C: Cr 63 SmC 39 I; ^{1}H NMR (CDCl$_3$) δ_H: 1.50–1.59 (4H, m), 1.71–1.79 (4H, m), 1.81–1.89 (4H, m), 2.40 (4H, t), 4.03 (4H, t), 5.23 (4H, dt), 5.30 (4H, dt), 5.73 (2H, tt), 5.80–5.88 (4H, m), 6.96 (2H, d, *J*=8.7 Hz), 7.04 (1H, dd, *J*=2.5, 9.0 Hz), 7.31 (1H, d, *J*=2.5 Hz), 7.90 (1H, d, *J*=8.7 Hz), 7.96 (2H, d, *J*=8.7 Hz); IR ν_{max}/cm^{-1}: 3087, 2944, 2870, 1737, 1641, 1607, 1574, 1520, 1488, 1456, 1306, 1251, 1172, 987, 924, 830; MS (*m/z*) (EI): 604 (M+1), 521, 422, 312, 243, 115, 97, 83, 67 (M100); Elemental analysis, expected: C 69.63, H 6.84, N 2.32, S 5.31, obtained: C 69.69, H 7.05, N 2.29, S 5.11%.

4.5. 6-[7-(1-Vinylallyloxycarbonyl)heptyloxy]-2-{4-[7-(1-vinylallyloxycarbonyl)heptyloxy]phenyl}benzothiazole (BTHAZ-3)

The experimental procedure was as described for the preparation of compound **BTHAZ-2**. Transition temp. /°C: Cr 55 SmC 64 I; ^{1}H NMR (CDCl$_3$) δ_H: 1.34–1.56 (12H, m), 1.67 (4H, quint), 1.77–1.85 (4H, m), 2.36 (4H, t), 4.02 (4H, t), 5.23 (4H, dt), 5.30 (4H, dt), 5.73 (2H, tt), 5.80–5.88 (4H, m), 6.96 (2H, d, *J*=8.7 Hz), 7.04 (1H, dd, *J*=2.5, 9.0 Hz), 7.32 (1H, d, *J*=2.5 Hz), 7.88 (1H, d, *J*=8.7 Hz), 7.96 (2H, d, *J*=8.7 Hz); IR ν_{max}/cm^{-1}: 3060, 2945, 2870, 1737, 1640, 1610, 1572, 1520, 1488, 1454, 1310, 1250, 1172, 988, 924, 830; MS (*m/z*) (EI): 660 (M+1), 576, 510, 450, 243, 97, 83, 67 (M100); Elemental analysis, expected: C 70.99, H 7.48, N 2.12, S 4.86; obtained: C 71.13, H 7.78, N 2.11, S 4.64%.

4.6. 6-[10-(1-Vinylallyloxycarbonyl)decyloxy]-2-{4-[10-(1-vinylallyloxycarbonyl)decyloxy]phenyl}benzothiazole (BTHAZ-4)

The experimental procedure was as described for the preparation of compound **BTHAZ-2**. Transition temp. /°C: Cr 49 SmC 71 I; ^{1}H NMR (CDCl$_3$) δ_H: 1.27–1.41 (20H, m), 1.42–1.51 (4H, m), 1.60–1.68 (4H, m), 1.74–1.85 (4H, m), 2.34 (4H, t), 4.01 (4H, t), 5.23 (4H, dt), 5.30 (4H, dt), 5.73 (2H, tt), 5.80–5.88 (4H, m), 6.96

(2H, d, $J=8.7$ Hz), 7.05 (1H, dd, $J=2.5$, 9.0 Hz), 7.30 (1H, d, $J=2.5$ Hz), 7.90 (1H, d, $J=8.7$ Hz), 7.95 (2H, d, $J=8.7$ Hz); IR v_{max}/cm^{-1}: 3080, 2944, 2872, 1735, 1640, 1605, 1574, 1520, 1488, 1450, 1308, 1250, 1172, 989, 924, 830; MS (*m/z*) (EI): 744 (M+1), 661, 426, 243, 149, 107, 95, 83, 67 (M100); Elemental analysis, expected: C 72.64, H 8.26, N 1.88, S 4.31, obtained: C 72.86, H 8.48, N 1.85, S 4.12%.

4.7. *1-[(S)-5-bromo-3-methylpentyl]-2-dimethyloxirane (4b)*

A solution of 77% *m*-chloroperbenzoic acid (28.1 g, 0.1324 mol) and DCM (150 cm^3) was added dropwise to a stirred, cooled (ice bath) solution of (*S*)-(+)-citronellyl bromide (**4a**) (25.0 g, 0.1142 mol) in DCM (250 cm^3) at a rate sufficient to maintain the temperature below 10°C. After the addition was complete the reaction mixture was stirred at r.t. for 15 h. The reaction mixture was filtered to remove precipitated *m*-chlorobenzoic acid and the filtrate washed with a dilute sodium hydrogensulphite solution (10%, 50 cm^3) and with a saturated sodium hydrogen sulphite solution (2 × 25 cm^3). The organic layer was washed with water (2 × 200 cm^3), dried (MgSO$_4$), filtered and concentrated under reduced pressure to yield a colourless oil (24.8 g, 92.4%). Purity: >99% (GC). ^{1}H NMR (CD$_2$Cl$_2$) δ_H: 0.93 (3H, d), 1.27 (3H, s), 1.32 (3H, s), 1.33–1.94 (7H, m), 2.72 (1H, t), 3.38–3.51 (2H, m). IR v_{max} /cm^{-1}: 2961, 2927, 2873, 1461, 1379, 1325, 1268, 1250, 1220, 1121, 873, 738. MS *m/z* (EI): 235 (M+1), 219, 191, 175, 158, 156, 139 (M100), 111, 97, 75, 69. $[\alpha]_d^{20} = +2.40°$.

4.8. *(S)-6-Bromo-4-methylhexanal (4c)*

Periodic acid (23.9 g, 0.1049 mol) was added portionwise to compound **4b** (22.0 g, 0.0936 mol) in THF (dry, 500 cm^3) at r.t. The reaction mixture was stirred for 45 min and quenched with water (500 cm^3). THF was removed *in vacuo* and the aqueous layer extracted with diethyl ether (3 × 100 cm^3), dried (MgSO$_4$), filtered and concentrated under reduced pressure. The crude product was purified by gravity column chromatography (silica gel, ethyl acetate/hexane, 10/90%) to yield a colourless oil (11.8 g, 65.2%). Purity: 96% (GC). ^{1}H NMR (CDCl$_3$) δ_H: 0.92 (3H, d), 1.40–1.93 (5H, m), 2.40–2.53 (2H, m), 3.38–3.49 (2H, m), 9.79 (1H, t, –CHO). IR v_{max} /cm^{-1}: 2959, 2931, 2872, 1726, 1461, 1381, 1355, 1256, 1127, 1048, 735. MS *m/z* (EI): 194, 192 (M$^+$), 177, 159, 149, 113, 95 (M100), 83, 69.

4.9. *(S)-6-Bromo-4-methylhexanoic acid (4d)*

Jones reagent [CrO$_3$ (7.00 g), conc. H$_2$SO$_4$ (2.50 cm^3), H$_2$O (40 cm^3)] was added dropwise to a solution of compound **4c** (5.00 g, 0.0259 mol) in acetone (30 cm^3) at 0°C at such a rate as to maintain the temperature of the solution below 10°C. Upon completion of the oxidation, monitored by GC, propan-2-ol (20 cm^3) was added and the reaction mixture stirred at r.t. for 15 min. The reaction mixture was then poured onto water (100 cm^3) and extracted into diethyl ether (3 × 100 cm^3). The combined ethereal extracts were washed with brine (100 cm^3), water (2 × 100 cm^3), dried (MgSO$_4$), filtered and concentrated under reduced pressure. The residue was purified by gravity column chromatography (silica gel, ethyl acetate/hexane, 10/90%) to yield a colourless oil (3.75 g, 69.3%). Purity: 96% (GC). ^{1}H NMR (CDCl$_3$) δ_H: 0.93 (3H, d), 1.44–1.93 (5H, m), 2.32–2.46 (2H, m), 3.39–3.48 (2H, m), 10.82 (1H, s, –COOH). IR v_{max} / cm^{-1}: 2550–3000, 1710, 1440, 1381, 1357, 1283, 1119, 1050, 735. MS *m/z* (EI): 210, 208 (M$^+$), 191, 149, 129, 111, 101, 83, 69 (M100).

4.10. *1,4-Pentadien-3-yl (S)-6-bromo-4-methylhexanoate (4e)*

DCC (3.45 g, 0.0167 mol) was added to a stirred solution of compound **4d** (3.50 g, 0.0167 mol), 1,4-pentadien-3-ol (1.41 g, 0.0167 mol) and DMAP (2.04 g, 0.0167 mol) in DCM (100 cm^3) at r.t. The reaction mixture was stirred overnight. The by-product, dicyclohexylurea, was filtered off, the filtrate concentrated under reduced pressure and then purified by gravity column chromatography (silica gel, DCM/hexane, 50/50%), to yield a pale yellow oil (4.10 g, 65.6%). The product was distilled under reduced pressure to yield a colourless oil (3.10 g, 67.2%). B.p./°C: 80–86, 1 mmHg. Purity: >99% (GC). ^{1}H NMR (CDCl$_3$) δ_H: 0.91 (3H, d), 1.46–1.93 (5H, m), 2.30–2.45 (2H, m), 3.36–3.50 (2H, m), 5.23 (2H, dt), 5.30 (2H, dt), 5.72 (1H, tt), 5.80–5.88 (2H, m). IR v_{max} /cm^{-1}: 3100, 3030, 2928, 2854, 1739, 1650, 1465, 1250, 1181, 983, 931, 725. MS *m/z* (EI): 276, 274 (M$^+$), 261, 259, 247, 245, 193, 127, 93, 83 (M100), 67. Elemental analysis, expected: C 52.38, H 6.96; obtained: C 52.22, H 6.97%.

4.11. *6-[(S)-3-Methyl-5-(1-vinylallyloxycarbonyl)pentyloxy]-2-{4-[(S)-3-methyl-5-(1-vinylallyloxycarbonyl) pentyloxy]phenyl}benzothiazole (BTHAZ-5)*

A mixture of 2-(4-hydroxyphenyl)-5-hydroxybenzothiazole (0.30 g, 0.0012 mol), 1,4-pentadien-3-yl

(S)-6-bromo-4-methylhexanoate, (0.78 g, 0.0028 mol) and potassium carbonate (0.51 g, 0.0037 mol) in DMF (10 cm³) was heated at 90 °C for 48 h. The reaction mixture was cooled to r.t., water (50 cm³) was added and the product extracted into DCM (2 × 100 cm³). The combined organic layers were washed with brine (4 × 100 cm³), dried (MgSO₄), filtered and concentrated under reduced pressure. The crude product was purified by gravity column chromatography (silica gel, ethyl acetate/hexane, 20/80%) to yield a colourless oil which crystallized overnight (0.35 g, 44.9%). Transition temp. /°C: Cr 53 SmC* 62 I. ^{1}H NMR (CDCl₃) δ_H: 0.97 (3H, d), 0.99 (3H, d), 1.50–1.91 (10H, m), 2.34–2.49 (4H, m), 4.03–4.09 (4H, m), 5.23 (4H, dt), 5.30 (4H, dt), 5.73 (2H, tt), 5.80–5.88 (4H, m), 6.95 (2H, d, J=8.7 Hz), 7.05 (1H, dd, J=2.5, 9.0 Hz), 7.32 (1H, d, J=2.5 Hz), 7.89 (1H, d, J=8.7 Hz), 7.96 (2H, d, J=8.7 Hz). IR v_{max}/cm⁻¹: 3087, 2957, 2932, 2874, 1736, 1641, 1608, 1574, 1524, 1491, 1456, 1307, 1254, 1172, 985, 929, 834. MS (m/z) (EI): 632 (M+1), 549, 436, 243, 129, 111, 91, 83, 67 (M100). Elemental analysis; expected: C 70.56, H 6.88, N 2.22, S 5.09; obtained: C 70.81, H 7.07, N 2.26, S 4.84%.

Acknowledgements

References

[1] S.M. Kelly. *Flat Panel Diplays, Advanced Organic Materials,* RSC materials monographs (2000).
[2] C.H. Chen, J. Shi, C.W. Tang. *Coord. Chem. Rev.*, **171**, 161 (1998).
[3] R.H. Friend, R.W. Gymer, A.B. Holmes, J.H. Burroughes, R.N. Marks, C. Taliani, D.D.C. Bradley, D.A. Dos Santos, J.L. Brédas, M. Lögdlund, W.R. Salaneck. *Nature*, **397**, 121 (1999).
[4] A. Kraft, A.C. Grimsdale, A.B. Holmes. *Angew. Chem. int. Ed. Engl.*, **37**, 402 (1998).
[5] C.D. Müller, A. Falcou, N. Reckefuss, M. Rojahn, V. Wiederhim, P. Rudati, H. Frohne, O. Nuykens, H. Becker, K. Meerholz. *Nature*, **421**, 829 (2003).
[6] M. Remmers, D. Neher, G. Wegner. *Macromol. Chem. Phys.*, **198**, 2551 (1997).
[7] X.C. Li, T.M. Yong, J. Gruener, A.B. Holmes, S.C. Moratti, F. Cacialli, R.H. Friend. *Synth. Met.*, **84**, 437 (1997).
[8] G. Klärner, J.-I. Lee, V.Y. Lee, E. Chan, J.P. Chen, A. Nelson, D. Markiewicz, R. Siemens, J.C. Scott, R.D. Miller. *Chem. Mater.*, **11**, 1800 (1999).
[9] E. Bellman, S.E. Shaheen, S. Thayumanavan, S. Barlow, R.H. Grubbs, S.R. Marder, B. Kippelen, N. Peyghambarian. *Chem. Mater.*, **10**, 1668 (1998).
[10] A.P. Davey, R.G. Howard, W.J. Blau. *J. mater. Chem.*, **7**, 417 (1997).
[11] M. Grell, D.D.C. Bradley. *Adv. Mater.*, **11**, 895 (1999).
[12] C. Sánchez, B. Villacampa, R. Alcalá, C. Martinez, L. Oriol, M. Pinol, J.L. Serrano. *Chem. Mater.*, **11**, 2804 (1999).
[13] C. Sánchez, B. Villacampa, R. Cases, R. Alcalá. *J. appl. Phys.*, **87**, 274 (2000).
[14] N. Yoshimoto, J.-I. Hanna. *J. Mater. Chem.*, **13**, 1004 (2003).
[15] A. Bacher, P.G. Bentley, D.D.C. Bradley, L.K. Douglas, P. Glarvey, M. Grell, K.S. Whitehead, M. Turner. *J. mater. Chem.*, **9**, 2985 (1999).
[16] A.E.A. Contoret, S.R. Farrar, P.O. Jackson, L. May, M. O'neill, J.E. Nicholls, S.M. Kelly, G.J. Richards. *Adv. Mater.*, **12**, 971 (2000).
[17] A.E.A. Contoret, S.R. Farrar, M. O'Neill, J.E. Nicholls, G.J. Richards, S.M. Kelly, A.W. Hall. *Chem. Mater.*, **14**, 1477 (2002).
[18] M.P. Aldred, A.J. Eastwood, S.M. Kelly, P. Vlachos, A.E.A. Contoret, S.R. Farrar, B. Mansoor, M. O'Neill, W. Chung Tsoi. *Chem. Mater.*, **16**, 4928 (2004).
[19] M. O'Neill, S.M. Kelly. *Adv. Mater.*, **15**, 1135 and references therein (2003).
[20] S.R. Farrar, A.E.A. Contoret, M. O'Neill, J.E. Nicholls, G.J. Richards, S.M. Kelly. *Phy. Rev. B*, **66**, 125107 (2002).
[21] A.E.A. Contoret, S.R. Farrar, S.M. Khan, M. O'Neill, G.J. Richards, M.P. Aldred, S.M. Kelly. *J. appl. Phys.*, **93**, 1465 (2003).
[22] M. Jandke, D. Hanft, P. Strohriegel, K. Whitehead, M. Grell, D.D.C. Bradley. *Proc. SPIE.*, **4105**, 338 (2001).
[23] P. Strohriegel, D. Hanft, M. Jandke, T. Pfeuffer. *Mat. Res. Soc. Symp. Proc.*, **709**, 31 (2002).
[24] M. Funahashi, J.I. Hanna. *Appl. Phys. Lett.*, **73**, 3733 (1998).
[25] M. Funahashi, J.I. Hanna. *Appl. Phys. Lett.*, **76**, 2574 (2000).
[26] P. Vlachos, S.M. Kelly, B. Mansoor, M. O'Neill. *Chem. Commun.*, 874 (2002).
[27] A.W. Grice, A. Tajbakhsh, P.L. Burn, D.D.C. Bradley. *Adv. Mater.*, **9**, 1174 (1997).
[28] R. Fink, C. Frenz, M. Thelakkat, H.-W. Schmidt. *Macromolecules*, **30**, 8177 (1997).
[29] R. Fink, Y. Heischkel, M. Thelakkat, H.-W. Schmidt. *Chem. Mater.*, **10**, 3620 (1998).
[30] T.-H. Huang, J.T. Lin. *Chem. Mater.*, **16**, 5387 (2004).
[31] D. Adam, P. Schuhmacher, J. Simmerer, L. Häußling, W. Paulus, K. Siemensmeyer, K.-H. Etzbach, H. Ringsdorf, D. Haarer. *Adv. Mater.*, **7**, 276 (1995).
[32] M.P. Aldred, M. Carrasco-Orozco, A.E.A. Contoret, D. Dong, S.R. Farrar, S.M. Kelly, S.P. Kitney, D. Mathieson, M. O'Neill, W.-C. Tsoi, P. Vlachos, K.L. Woon, *J. mater. Chem.* (submitted).
[33] R.D. Stephens, C.E. Castro. *J. org. Chem.*, **23**, 3313 (1963).
[34] G.W. Gray, M. Hird, D. Lacey, K.J. Toyne. *J. chem. Soc., Perkin Trans.*, **2**, 2041 (1989).
[35] A. Suzuki. *Pure appl. Chem.*, **66**, 213 (1994).
[36] J.F. McOmie, M.L. Watts, D.E. West. *Tetrahedron*, **24**, 2289 (1968).
[37] G.R. Richards. Ph.D. Thesis, University of Hull (2000).
[38] B. Neisses, W. Steglich. *Angew Chem. Int. Ed. Engl.*, **17**, 522 (1978).

[39] J.F. Geldard, F. Lions. *J. org. Chem.*, **30**, 318 (1965).
[40] J. Spychala. *Synth. Commun.*, **30**, 1083 (2000).
[41] I.P. Buxton, A.W. Hall, D. Lacey. *Macromol. Chem. Phys.*, **198**, 2307 (1997).
[42] M. Funahashi, J.-I. Hanna. *Jpn. J. appl. Phys.*, **35**, L703 (1996).
[43] M. Funahashi, J.-I. Hanna. *Phys. Rev. Lett.*, **78**, 2184 (1997).
[44] M. Funahashi, J.-.I. Hanna. *Mol. Cryst. liq. Cryst.*, **304**, 429 (1997).
[45] R.L. Mital, S.K. Jain. *J. chem. Soc.*, 2148 (1969).
[46] P. Vlachos. Ph.D. Thesis, University of Hull (2003).
[47] G.J. Cernigliaro, P.J. Kocienski. *J. org. Chem.*, **42**, 3622 (1977).
[48] M.F. Boehm, G.D. Prestwich. *J. org. Chem.*, **51**, 5447 (1986).
[49] C.E. Holloway, S.A. Kandil, I.M. Walker. *J. Am. chem. Soc.*, **94**, 4024 (1972).
[50] A.J. Fatiadi. *Synthesis*, 85 (1987).
[51] K. Bowden, I.M. Heilbron, E.R.H. Jones, B.C.L. Weedon. *J. chem. Soc.*, 39 (1946).
[52] J. Raimundo, P. Blanchard, H. Brisset, S. Akoudad, J. Roncali. *Chem. Commun.*, 939 (2000).
[53] C. Kitamura, S. Tanaka, Y. Yamashita. *Chem. Mater.*, **8**, 570 (1996).
[54] M. Ranger, M. Leclerc. *Macromolecules*, **32**, 3306 (1999).
[55] K. Pilgram, M. Zupan, R. Skiles. *J. heterocycl. Chem.*, **7**, 629 (1970).